Activation of invariant natural killer T cells by lipid excess promotes tissue inflammation, insulin resistance, and hepatic steatosis in obese mice

Lan Wu[a,1,2], Vrajesh V. Parekh[a,1], Curtis L. Gabriel[a,3], Deanna P. Bracy[b,c], Pamela A. Marks-Shulman[d], Robyn A. Tamboli[d], Sungjune Kim[a,4], Yanice V. Mendez-Fernandez[a,3], Gurdyal S. Besra[e], Jefferson P. Lomenick[f], Brandon Williams[d], David H. Wasserman[b,c], and Luc Van Kaer[a,1,2]

Departments of [a]Microbiology and Immunology, [b]Molecular Physiology and Biophysics, and [d]Surgery, [f]Division of Endocrinology, Department of Pediatrics, and [c]Vanderbilt–National Institutes of Health Mouse Metabolic Phenotyping Center, Vanderbilt University School of Medicine, Nashville, TN 37232; and [e]School of Biosciences, University of Birmingham, Edgbaston, Birmingham B15 2TT, United Kingdom

Edited* by Peter Cresswell, Yale University School of Medicine, New Haven, CT, and approved March 19, 2012 (received for review January 10, 2012)

Obesity triggers a low-grade systemic inflammation, which plays an important role in the development of obesity-associated metabolic diseases. In searching for links between lipid accumulation and chronic inflammation, we examined invariant natural killer T (iNKT) cells, a subset of T lymphocytes that react with lipids and regulate inflammatory responses. We show that iNKT cells respond to dietary lipid excess and become activated before or at the time of tissue recruitment of inflammatory leukocytes, and that these cells progressively increase proinflammatory cytokine production in obese mice. Such iNKT cells skew other leukocytes toward proinflammatory cytokine production and induce an imbalanced proinflammatory cytokine environment in multiple tissues. Further, iNKT cell deficiency ameliorates tissue inflammation and provides protection against obesity-induced insulin resistance and hepatic steatosis. Conversely, chronic iNKT cell stimulation using a canonical iNKT cell agonist exacerbates tissue inflammation and obesity-associated metabolic disease. These findings place iNKT cells into the complex network linking lipid excess to inflammation in obesity and suggest new therapeutic avenues for obesity-associated metabolic disorders.

cluster of differentiation 1d | glycolipid-reactive T cells | alpha-galactosylceramide | obesity-induced inflammation

Obesity and its associated metabolic sequelae, notably insulin resistance and hepatic steatosis, have emerged as a group of metabolic disorders in which a low-grade chronic inflammation plays an important role in disease pathogenesis (1–4). The innate branch of the immune system is activated during obesity. One aspect of this activation is recruitment of tissue macrophages (5, 6). Release of proinflammatory cytokines from multiple tissues in obesity creates a low-grade systemic inflammation that interferes with metabolic pathways (1–3). Recently, studies have revealed involvement of the adaptive branch of the immune system, namely, B lymphocytes and the antibodies they produce and T lymphocytes, such as $CD8^+$ effector T cells, in obesity-triggered inflammation and have suggested a causal role of these adaptive immune components in activating innate immunity (7–10). Despite these advances, the cellular and molecular mechanisms that link lipid accumulation and tissue inflammation in obesity remain to be defined (1).

Several subsets of T lymphocytes play fundamental roles in recognizing inflammation-associated stimuli and orchestrating inflammatory responses. The $CD4^+CD25^+Foxp3^+$ regulatory T (T_{reg}) cells generally play a suppressive role in inflammatory diseases, and these cells have been shown to protect obese mice against excessive inflammation (9). Another subset of T cells, endowed with potent immunomodulatory functions, is natural killer T (NKT) cells (11–13). Unlike conventional T cells, which recognize peptides, NKT cells react to lipid stimuli. On activation, NKT cells produce a variety of immunomodulatory cytokines, including proinflammatory cytokines, such as IFN-γ and TNF-α, and antiinflammatory cytokines, such as IL-4 and IL-10. NKT cell-derived cytokines interact with and influence the function of multiple cell types of the immune system, including conventional T and B cells, macrophages, and dendritic cells (DCs) (13, 14). Through these interactions, NKT cells can shape subsequent inflammatory responses and influence disease outcomes. NKT cells are enriched in liver and are present in spleen, peripheral blood, and white adipose tissue (WAT) (15, 16).

NKT cells are composed of several subpopulations (17). The major subpopulation, referred to as invariant NKT (iNKT) cells, expresses a semiinvariant T-cell receptor (TCR) (17). This TCR is specific for lipid antigens bound by the antigen-presenting molecule CD1d (11–13, 18). Although iNKT cells can be directly activated by exogenous lipid antigens presented by CD1d on antigen-presenting cells (APCs), these cells can also be activated by indirect means (13, 14). iNKT cells readily react to their specific agonist α-galactosylceramide (α-GalCer) and can be unambiguously identified by α-GalCer–loaded CD1d-tetramers (α-GalCer/CD1d-tetramers) (19). Another subpopulation of NKT cells, termed variant NKT (vNKT) cells, has a more diverse TCR repertoire but shares several features with iNKT cells (13, 20).

Evidence in the literature suggests that obesity has an impact on NKT cells. Early studies collectively reported reductions in the proportion of hepatic NKT cells during obesity in mice but did not examine their function, and interpreted these observations as lipid-induced hepatic NKT cell depletion leading to compromised protection of these cells against hepatic steatosis (21–25). However, a recent study argued for a pathogenic role of NKT cells in high-fat diet (HFD)-induced WAT inflammation, using β2-microglobulin–deficient mice (26), which, in addition to lacking all subsets of NKT cells, lack several other types of leukocytes, notably $CD8^+$ T cells (8, 27). As such, the functional

Author contributions: L.W., D.H.W., and L.V.K. designed research; L.W., V.V.P., C.L.G., D.P.B., P.A.M.-S., R.A.T., S.K., Y.V.M.-F., J.P.L., and B.W. performed research; G.S.B. contributed new reagents/analytic tools; L.W., V.V.P., C.L.G., D.H.W., and L.V.K. analyzed data; and L.W., D.H.W., and L.V.K. wrote the paper.

The authors declare no conflict of interest.

*This Direct Submission article had a prearranged editor.

[1]Present address: Department of Pathology, Microbiology, and Immunology, Vanderbilt University School of Medicine, Nashville, TN 37232.

[2]To whom correspondence may be addressed. E-mail: lan.wu@vanderbilt.edu or luc.van.kaer@vanderbilt.edu.

[3]Present address: Department of Medicine, Vanderbilt University School of Medicine, Nashville, TN 37232.

[4]Present address: Department of Radiation Oncology, Moffitt Cancer Center, University of South Florida, Tampa, FL 33612.

This article contains supporting information online at www.pnas.org/lookup/suppl/doi:10.1073/pnas.1200498109/-/DCSupplemental.

status of NKT cells and, more specifically, iNKT cells and their role in the pathogenesis of obesity remain unclear. In this report, we have tested the hypothesis that lipid excess in obesity activates iNKT cells, which, in turn, promotes obesity-induced inflammation, insulin resistance, and hepatic steatosis.

Results

Early Activation of iNKT Cells by Dietary Lipid Excess. To examine whether iNKT cells can respond to lipid excess, we first used a diet-induced obesity (DIO) model by HFD feeding, in comparison to a low-fat diet (LFD) that was comparable to a regular chow diet (RCD). We focused on liver and WAT, two metabolic organs that accumulate excessive lipids and play critical roles in obesity-triggered inflammation. Whereas iNKT cells are enriched in liver (Fig. S1*A*) and hepatic iNKT cells have been extensively investigated, WAT iNKT cells have not been previously characterized at the cellular level in mice. Using α-GalCer/CD1d-tetramers, we detected iNKT cells in the stroma-vascular fractions (SVFs) from WAT of lean mice (Fig. S1*A*) that were absent in iNKT cell-deficient mice, and the proportion of these cells among all leukocytes was much higher than in spleen and peripheral blood (Fig. S1*A*). We then fed the test diets to mice for different durations and examined iNKT cells as well as several other cell types, including macrophages and effector CD8$^+$ T cells (Fig. S1*B*). Although the prevalence of hepatic iNKT cells among intrahepatic leukocytes (IHLs) was comparable between HFD- and LFD-fed mice within 1 wk of feeding, the percentage of these cells declined with continuous HFD feeding (Fig. 1*A*, *Upper*). On the other hand, although the prevalence of WAT iNKT cells tended to decline with increased age, percentages of these cells remained comparable between the two groups (Fig. 1*B*, *Upper*) and declined in the HFD-fed group after prolonged feeding (Fig. 1*C*). Because the HFD induces rises in body and organ weights as well as in IHL and SVF cells (Fig. S2*A*), we also quantified iNKT cell numbers per gram of tissue and observed no significant differences between the two diet groups after either 1 wk or 12 wk of feeding (Fig. S2*B*). Because activation of iNKT cells under a variety of pathological conditions is often accompanied by decreases in their proportions, the above observations could simply reflect iNKT cell activation induced by the HFD, which led us to investigate expression of activation markers. Both hepatic and WAT iNKT cells up-regulated the surface activation marker ICOS soon after initiation of HFD feeding, which was evident as early as 3 d after initiation of HFD feeding in WAT and slightly delayed in liver (Fig. 1 *A*, *Middle* and *B*, *Middle* and Fig. S1*C*) at a time when rises in liver weight, blood lipid triglycerides (TGs), cholesterol (CHO), and free fatty acids (FFAs) in HFD-fed mice were not yet observed (Fig. S2*A*). ICOS levels on iNKT cells from HFD-fed mice declined thereafter but remained slightly elevated for a prolonged period of time (Fig. 1 *A* and *B*, *Middle*). Further, iNKT cells of HFD-fed mice down-regulated surface NK1.1 expression, another indicator of iNKT cell activation (28) (Fig. 1 *A* and *B*, *Lower* and Fig. S1*D*). Although NK1.1 down-regulation appeared at later time points than ICOS up-regulation, its down-regulation was sustained. We did not consistently detect up-regulation of several other activation markers, including CD69, CD40L, and CD25, on iNKT cells of HFD-fed mice.

Consistent with previous reports (5–8), we detected increases in the percentages of macrophages and CD8$^+$ T cells in SVFs after prolonged HFD feeding (Fig. 1*E*). Increases in the prevalence of macrophages and CD8$^+$ T cells were consistent with increases in the total numbers of cells per organ and numbers of cells per gram of tissue (Fig. S2*C*). Among CD8$^+$ T cells, CD44$^+$CD62L$^-$ effector T cells were preferentially increased in obese mice (Fig. 1*F*, *Right*).

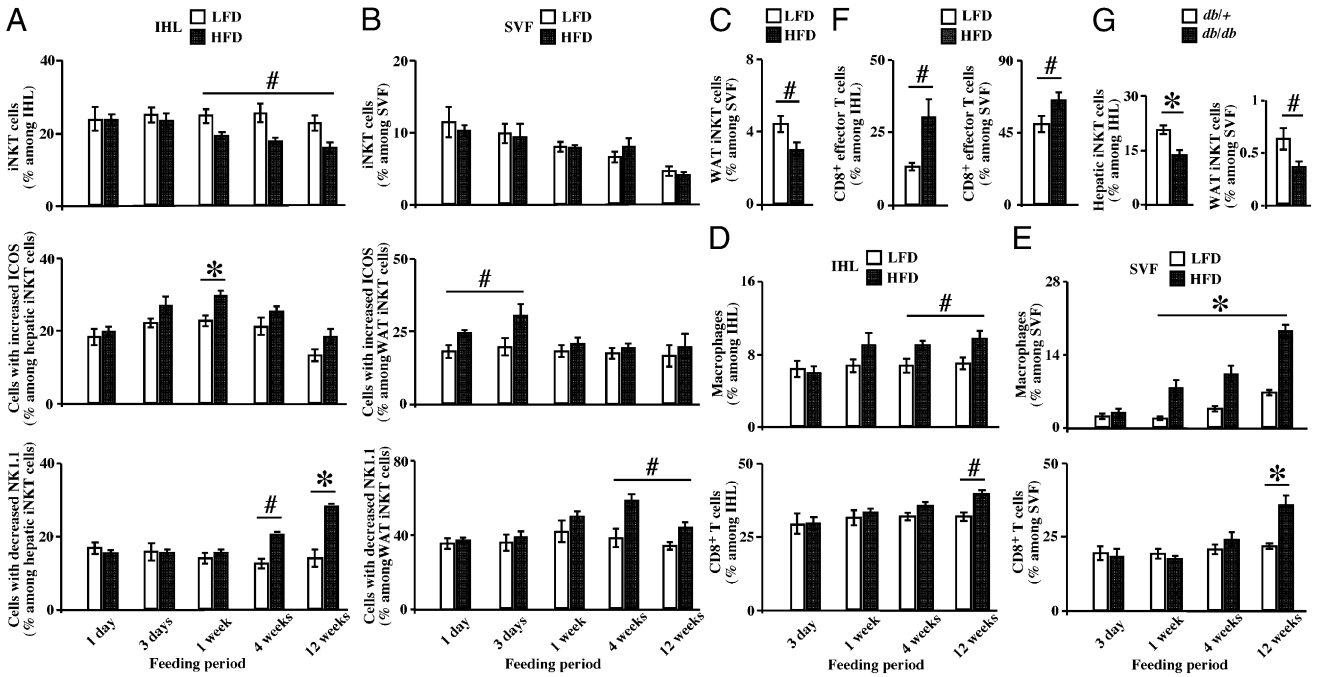

Fig. 1. Evidence for iNKT cell activation and increases in macrophages and CD8$^+$ T_{eff} cells in liver and WAT of HFD-fed mice and for numerical changes in hepatic and WAT iNKT cells in *db*/*db* mice. (*A* and *B*) Male WT B6 mice were fed test diets for the durations indicated. IHLs and SVFs were labeled and analyzed by flow cytometry. Percentage of iNKT cells among IHLs (*A*) or SVFs (*B*) and percentage of iNKT cells with increased ICOS or decreased NK1.1 among hepatic iNKT cells (*A*) and WAT iNKT cells (*B*) are shown. Gating strategies and representative flow cytometric plots are shown in Fig. S1. (*C*) Male WT B6 mice were fed test diets for 20 wk and used for labeling of iNKT cells among SVFs. Macrophages and CD8$^+$ T cells among IHLs (*D*) or SVFs (*E*) were examined. (*F*) CD44$^+$CD62L$^-$CD8$^+$ T cells among IHLs or SVFs were examined after 12 wk of feeding. Combined data from two to three independent experiments are shown (1 d, 3 d, and 4 wk: $n = 10$; 1 wk and 12 wk: $n = 15$; 20 wk: $n = 5$). (*G*) *db*/*db* and *db*/$^+$ mice on the B6 background were fed the RCD. Mice were analyzed at 15 wk of age for iNKT cells among IHLs and SVFs. Combined data from two independent experiments (*db*/$^+$, $n = 5$; *db*/*db*, $n = 7$) are shown. $^{\#}P < 0.05$; $^{*}P < 0.01$.

We found that such recruitment of inflammatory cells was not limited to WAT, because IHLs of HFD-fed obese mice showed similar alterations, albeit to a lesser degree and at later time points than in WAT (Fig. 1 *D* and *F*, *Left* and Fig. S2*C*). We compared the appearance of these inflammatory cells with the kinetics of iNKT cell activation in liver and WAT during HFD feeding. Our results indicated that HFD-induced inflammation occurred earlier in WAT than in liver and that iNKT cell activation occurred before or at the time of recruitment of macrophages and $CD8^+$ effector T cells in both liver and WAT (Fig. 1 *A*, *B*, *D*, and *E*). Both male and female mice underwent similar changes, although their occurrence in females was somewhat delayed.

iNKT Cells Promote a Proinflammatory Cytokine Environment in Obese Mice. Activated iNKT cells produce a mixture of pro- and antiinflammatory cytokines, which is dictated by the nature and magnitude of the stimuli received, and subsequently influences immune responses mediated by other leukocytes (11–13, 18). We therefore analyzed the cytokine profile of iNKT cells by intracellular staining (Fig. S3*A*). After 12 wk of feeding, hepatic iNKT cells produced increased levels of several cytokines, including IFN-γ, IL-4, and TNF-α, both under basal conditions and following in vivo challenge with α-GalCer (Fig. 2 *A* and *B*). Similar alterations were also observed after short-term HFD feeding, albeit to a lesser extent (Fig. S3 *B* and *C*). These findings suggest that dietary lipid excess promotes hyperresponsiveness in iNKT cells, leading to increased production of cytokines, such as TNF-α, that play a pathogenic role in obesity-induced metabolic disease (1–4).

We next examined the impact of the above iNKT cell alterations on cytokine production from other leukocytes within liver. For this purpose, we measured cytokines in the supernatant of

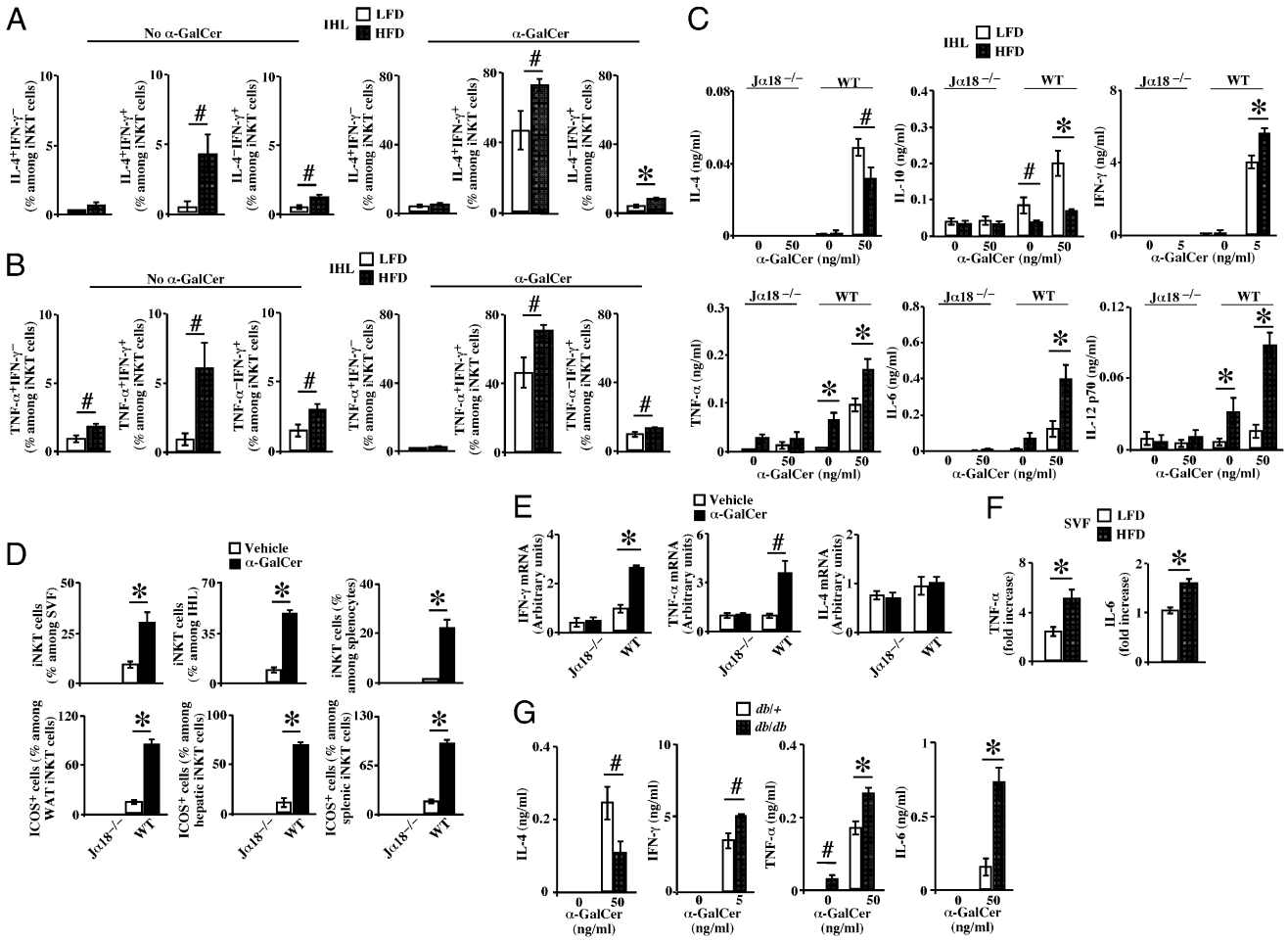

Fig. 2. Cytokine profile of iNKT cells, IHLs, and SVFs after prolonged HFD feeding and cytokine production from ex vivo cultured IHLs of *db/db* mice. (*A* and *B*) Male WT B6 mice were fed test diets for 12 wk. They were either left unchallenged or injected i.p. with α-GalCer at 50 ng/g of body weight and killed 2 h later. The percentage of cells stained for the indicated cytokines among gated hepatic iNKT cells was examined. Shown are statistical analyses of representative data from two independent experiments using four to five mice in each group per experiment. Gating strategies and representative flow cytometric plots are shown in Fig. S3*A*. (*C*) Mice were fed test diets for 12 wk. IHLs from mice of the indicated genotypes were cultured ex vivo for 72 h. Cytokines in the supernatants were determined by ELISA. Combined data from three independent experiments are shown (LFD, $n = 8$; HFD, $n = 10$). Ten-week-old mice of the indicated genotypes on the RCD diet were injected i.p. with vehicle or α-GalCer (1 μg per mouse) and killed 3 d later for analyses of iNKT cells (*D*; $n = 5$ in each treatment group) and of cytokines in WAT by real-time PCR (*E*; representative results from 2 independent experiments using 3–4 mice in each group per experiment). (*F*) Male WT B6 mice were fed test diets for 12 wk. Leukocytes were purified from SVFs by flow cytometric cell sorting and cultured ex vivo for 72 h in the absence or presence of 50 ng/mL α-GalCer. Cytokines in the supernatants were analyzed by ELISA. Results are presented as ratios of cytokine in the presence of α-GalCer/cytokine in the absence of α-GalCer (fold increase). Combined data from two independent experiments using two to three obese mice and six to nine lean mice in each group per experiment are shown. (*G*) *db/db* and *db/*$^+$ mice on the B6 background were fed the RCD. Mice were analyzed at 15 wk of age. IHLs were cultured ex vivo for 72 h for cytokine analyses in the supernatants by ELISA. Combined data from two independent experiments (*db/*$^+$, $n = 5$; *db/db*, $n = 7$) are shown. $^{\#}P < 0.05$; $^{*}P < 0.01$.

IHLs cultured ex vivo in the absence or presence of α-GalCer. The cytokines in the supernatant of these cultures reflect the total cytokines produced by iNKT cells themselves and by other cell types stimulated in trans by the activated iNKT cells. After 12 wk of feeding, although IL-4 was undetectable in the absence of α-GalCer in IHL cultures from either HFD- or LFD-fed mice, it was lower in α-GalCer–stimulated IHLs of HFD-fed mice (Fig. 2*C*, *Upper Left*). Under basal conditions, IHLs of HFD-fed obese mice produced increased levels of IL-12 and TNF-α but decreased levels of IL-10 (Fig. 2*C*). Notably, stimulation of iNKT cells by α-GalCer further skewed IHLs toward proinflammatory cytokine production (Fig. 2*C*). These alterations in the cytokine production profile were also observed after short-term HFD feeding (Fig. S3*D*) and persisted with continuous feeding (Fig. S3*E*). The decreased levels of IL-4 and IL-10 in the IHL cultures of HFD-fed mice were unlikely caused solely by the reduced prevalence of iNKT cells among IHLs, because similar results were obtained for splenocytes, where the percentages of iNKT cells were comparable between HFD- and LFD-fed mice (Fig. S4 *A* and *B*). Of note, although iNKT cell dysfunction in mice with DIO was not limited to liver and WAT, such changes were less profound in other organs, such as spleen (Fig. S4 *B* and *C*).

We used the same strategy to analyze WAT iNKT cells but were unable to obtain consistent results, likely attributable to technical limitations, such as collagenase digestion and the heterogeneous cell populations in SVFs. We therefore took several alternative approaches. First, we assessed whether WAT iNKT cells could respond to specific stimuli. We injected adult lean mice with α-GalCer and found significant iNKT cell expansion in WAT accompanied by dramatic up-regulation of ICOS (Fig. 2*D*). WAT iNKT cells were as responsive to such an acute α-GalCer challenge as their counterparts in both liver and spleen (Fig. 2*D*). Second, we examined whether acute stimulation of iNKT cells by α-GalCer influenced the cytokine environment in WAT and observed a biased proinflammatory cytokine profile in α-GalCer–treated mice (Fig. 2*E*). Third, we chronically stimulated iNKT cells with α-GalCer in the context of HFD feeding and detected elevated TNF-α and IFN-γ in iNKT cells (see Fig. 6 *D* and *E*). Finally, we purified leukocytes from SVFs by flow cytometric cell sorting based on their forward scatter (FSC)/side scatter (SSC) distribution, cultured these cells in the absence or presence of α-GalCer, and measured cytokine responses. The results showed that SVF leukocytes from HFD-fed mice secreted higher amounts of TNF-α and IL-6 in response to α-GalCer (Fig. 2*F*). We were unable to detect IL-4 in any of these cultures. Taken together, the results presented thus far indicate that iNKT cells rapidly respond to dietary lipid excess and produce increased levels of proinflammatory cytokines. On further stimulation, these iNKT cells cause increased proinflammatory and decreased antiinflammatory cytokine production from other leukocyte populations in liver and WAT.

Functional Properties of iNKT Cells in *db/db* Mice Are Similar to Those of Mice with DIO. To provide further evidence that lipid excess chronically stimulates iNKT cells in obesity, we performed experiments in leptin receptor-deficient *db/db* mice, a genetic model of obesity. Compared with lean *db*/$^{+}$ controls, *db/db* mice developed obesity, hypercholesterolemia, and insulin resistance on the RCD similar to the DIO model (Fig. S2*D*). We observed that decreases in the proportions of hepatic and WAT iNKT cells in morbidly obese *db/db* mice resembled those of mice with DIO after prolonged feeding (Fig. 1*G*). The results from ex vivo cultured IHLs and splenocytes of *db/db* mice also resembled those obtained with the DIO model, with a biased cytokine production profile that became more pronounced on α-GalCer stimulation (Fig. 2*G* and Fig. S4 *D* and *E*). Collectively, our results in the DIO and *db/db* models provide evidence that lipid overabundance during excessive dietary lipid uptake or obesity chronically stimulates iNKT cells and increases their capacity to produce cytokines, which contributes to the generation of a proinflammatory cytokine environment in metabolically active organs.

iNKT Cell Deficiency Protects Against Obesity-Induced Insulin Resistance and Hepatic Steatosis. To investigate whether the observed alterations in iNKT cells play a role in obesity-associated metabolic disorders, we first took a loss-of-function approach. We used mice with DIO and *db/db* mice that were selectively deficient in iNKT cells [i.e., *Jα18*$^{-/-}$ mice (17)]. We fed the HFD or LFD to *Jα18*$^{-/-}$ mice and WT littermates. Although female *Jα18*$^{-/-}$ mice on the HFD gained weight slower than WT mice, both reached similar body weights after prolonged feeding (Fig. 3*A*). Our subsequent studies analyzed WT and *Jα18*$^{-/-}$ mice with a comparable degree of obesity (after 20–24 wk in females and after 10–12 wk in males). The absence of iNKT cells did not affect the levels of blood TGs or CHO (Fig. S5*A*), nor did it influence food intake or energy expenditure. Despite the minimal protection against weight gain and apparently no protection against hypercholesterolemia, the absence of iNKT cells protected against HFD-induced insulin resistance and excessive lipid accumulation. During an i.p. insulin tolerance test (IPITT), *Jα18*$^{-/-}$ mice on the HFD showed faster rates of glucose clearance (Fig. 3*B*). At sacrifice, these mice remained more insulin-sensitive, as reflected by a lower index of homeostasis model assessment of insulin resistance (HOMA-IR; Fig. 3*C*). The average size of WAT adipocytes was smaller in HFD-fed *Jα18*$^{-/-}$ mice (Fig. 3*D*). More importantly, these mice accumulated fewer lipids in their liver (Fig. 3 *E* and *F*). Consistent with the finding that J*α18*$^{+/-}$ mice have comparable numbers of iNKT cells as WT mice (17), HFD-fed *Jα18*$^{+/-}$ mice developed obesity, insulin resistance, and hepatic steatosis comparable to their WT littermates.

Next, we generated *db/db* mice lacking iNKT cells (i.e., *db/db*; *Jα18*$^{-/-}$ mice). We fed the RCD to these mice and compared them with *db/db* mice. The absence of iNKT cells did not affect body weight in either males or females (Fig. 3*G*), nor did it influence the levels of blood TGs and CHO (Fig. S5*B*). However, the protective effects of iNKT cell deficiency against insulin resistance in morbidly obese mice mirrored our findings in the DIO model (Fig. 3 *H* and *I*).

CD1d Deficiency Protects Against HFD-Induced Insulin Resistance and Hepatic Steatosis. We then sought to confirm our observations for iNKT cells and to evaluate the potential contribution of vNKT cells using *CD1d*$^{-/-}$ mice lacking both iNKT and vNKT cells (29). Similar to the *Jα18*$^{-/-}$ model, *CD1d*$^{-/-}$ mice had delayed HFD-induced weight gain in females (Fig. 4*A*). Reduced body weight in HFD-fed *CD1d*$^{-/-}$ mice was attributable to reduced fat accumulation (Fig. 4*B*), without significant influence on food intake or energy expenditure (Fig. S6*A*). After 12 wk of feeding, HFD-fed *CD1d*$^{-/-}$ mice showed better insulin sensitivity during a hyperinsulinemic-euglycemic clamp study (Fig. 4*C*). At sacrifice, when *CD1d*$^{-/-}$ and control mice had a comparable degree of obesity, *CD1d*$^{-/-}$ mice remained more insulin-sensitive (Fig. 4*D*). The HFD also induced less liver lipid accumulation in *CD1d*$^{-/-}$ mice (Fig. 4*E*). The results from *db/db* mice lacking iNKT and vNKT cells (*db/db*;*CD1d*$^{-/-}$ mice) that were fed the RCD mirrored our observations in the *db/db*;*Jα18*$^{-/-}$ model (Fig. 4 *F* and *G*). Collectively, our studies in the *CD1d*$^{-/-}$ model confirm the pathogenic role of iNKT cells in obesity-induced insulin resistance and hepatic steatosis.

iNKT Cell Deficiency Ameliorates Obesity-Induced Tissue Inflammation. Our earlier studies indicated that induction of activation markers on iNKT cells occurred before or at the time of rises in tissue macrophages (Fig. 1 *A*, *B*, *D*, and *E*). Because activated iNKT cells can interact with the latter cells (11–13), we examined whether the absence of iNKT cells influenced recruitment of these cells to

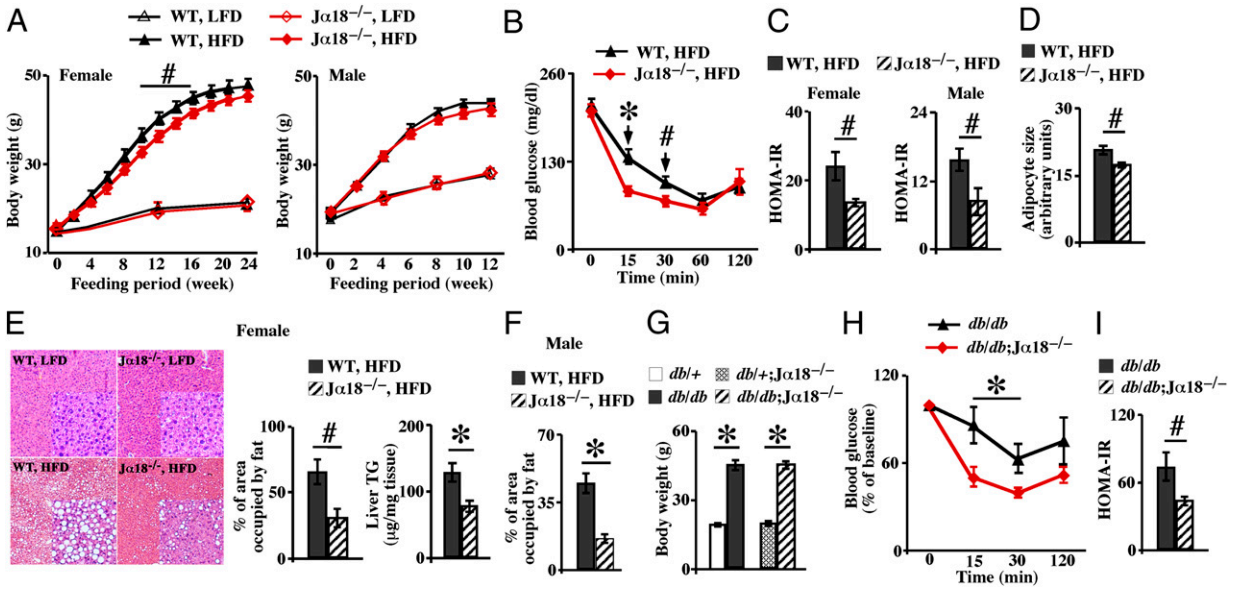

Fig. 3. Effects of iNKT cell deficiency on obesity-induced insulin resistance and hepatic steatosis in mice with DIO or genetic obesity. (*A*) Mice on the B6 background and of the indicated sex and genotypes were fed test diets for the durations indicated and were monitored for body weight gain. Results are a summary of more than three independent experiments ($n > 8$ in LFD groups, $n > 15$ in HFD groups). (*B*) Female mice of the indicated genotypes were fed the HFD for 20 wk and used for the IPITT. Results are a summary of two independent experiments (HFD-fed WT, $n = 8$; HFD-fed *Jα18*$^{-/-}$, $n = 7$). (*C*) Mice of the indicated sex and genotypes were fed test diets for 20 wk (female) or 10–12 wk (male) and killed at fasting state for measurements of HOMA-IR. Results are a summary of three independent experiments ($n = 10$). Mice of the indicated sex and genotypes were fed test diets for 20 wk (*D* and *E*) or 10–12 wk (*F*) and were killed for analyses of WAT adipocyte size (*D*) and liver lipids (*E* and *F*). (Magnification: *E*, 4×; *Insets*, 10×.) Results are a summary of three independent experiments (HFD-fed WT, $n = 10$; HFD-fed *Jα18*$^{-/-}$, $n = 8$). The *db*/$^{+}$ or *db/db* mice on the B6 background and of the indicated genotypes were fed the RCD, monitored for body weight (*G*), used for the IPITT at 12 wk of age (*H*), and killed at 15 wk of age for measurement of HOMA-IR (*I*). Results are a summary of three independent experiments (*db/db*, $n = 9$; *db/db;Jα18*$^{-/-}$, $n = 7$). $^{\#}P < 0.05$; $^{*}P < 0.01$.

metabolically active organs in obese mice. We fed the HFD to WT and *Jα18*$^{-/-}$ mice, and examined IHLs and SVF. Obese mice lacking iNKT cells accumulated significantly fewer macrophages in both liver and WAT (Fig. 5*A* and Fig. S7*A*). This reduction in macrophages in WAT was confirmed by immunocytochemistry of F4/80, as reflected by fewer crown-like structures in *Jα18*$^{-/-}$ animals (Fig. 5*B*). Although we did not observe differences in the proportions of T_{reg} cells among IHLs, SVF cells, and splenocytes comparing WT and *Jα18*$^{-/-}$ mice fed either of the diets for 8–10 wk, these cells appeared to be more suppressive in *Jα18*$^{-/-}$ mice fed the LFD (Fig. S7*B*), and such suppressive capacity was preserved in the HFD-fed *Jα18*$^{-/-}$ mice (Fig. 5*C*). Finally, because our earlier studies showed that the altered cytokine production capacity of iNKT cells skewed other leukocytes toward proinflammatory cytokine production in obese mice (Fig. 2), we investigated whether iNKT cells can influence the cytokine environment in metabolically active organs in obese mice. The HFD induced substantial elevations in TNF-α and monocyte chemoattractant protein-1 in liver and WAT of WT mice, and such elevations were less profound in *Jα18*$^{-/-}$ mice (Fig. 5 *D* and *E*), indicating that iNKT cells were activated in response to lipid excess exacerbate tissue inflammation. Additionally, the antiinflammatory, insulin-sensitizing, and fat-derived hormone adiponectin was expressed at significantly higher levels in WAT of iNKT cell-deficient mice compared with WT mice fed the HFD (Fig. 5*E*). Similar results were obtained for *CD1d*-deficient mice on the HFD (Fig. S6 *B* and *C*). Together, these results indicate that lipid excess-induced alterations in iNKT cell function promote tissue recruitment of macrophages and worsen proinflammatory responses in obese mice.

Chronic Treatment of HFD-Fed Mice with α-GalCer Exacerbates Tissue Inflammation, Insulin Resistance, and Hepatic Steatosis. The cytokine profile of iNKT cells influences subsequent inflammatory responses of other leukocytes, and hence the outcome of a variety of pathological conditions (11–13). This feature of iNKT cells has been extensively explored for therapeutic purposes (13). To complement our studies with iNKT cell-deficient mouse models with a gain-of-function approach, we examined the effects of repeated α-GalCer injection on inflammatory and metabolic parameters in HFD-fed mice. Although such treatment did not affect body weight (Fig. 6*A*), it significantly impaired insulin sensitivity (Fig. 6*B*) and exacerbated hepatic steatosis (Fig. 6*C*). Profound stimulation of hepatic and WAT iNKT cells was reflected by dramatic up-regulation of ICOS (Fig. 6 *D*, *Left* and *E*, *Left*), with further decreases in iNKT cell prevalence in liver and WAT (Fig. S8*A*). Further, these cells expressed higher levels of IFN-γ and TNF-α, even long after the last α-GalCer injection (Fig. 6 *D* and *E*). Consequently, more macrophages and $CD8^{+}$ T cells infiltrated liver and WAT (Fig. 6 *F* and *G*). Chronic α-GalCer treatment further depleted T_{reg} cells in WAT (Fig. 6*H* and Fig. S8*B*), but this was not evident in liver (Fig. S8*C*). Glycolipid C20:2, an analog of α-GalCer, has previously been shown to promote a T helper type 2 cytokine response in iNKT cells (30). We therefore examined whether chronic treatment with this reagent could influence HFD-induced metabolic disease but failed to observe significant effects against HFD-induced insulin resistance (Fig. S8*D*), whereas α-GalCer exacerbated HFD-induced insulin resistance in parallel studies.

Discussion

It has been increasingly recognized that low-grade systemic inflammation plays an important role in the pathogenesis of obesity-associated metabolic diseases (1, 3). This field has also begun to delineate the underlying mechanisms that initiate and sustain chronic inflammation in obesity. Although many unanswered questions remain, it is evident that both the innate and adaptive branches of the immune system are involved (31, 32). Our

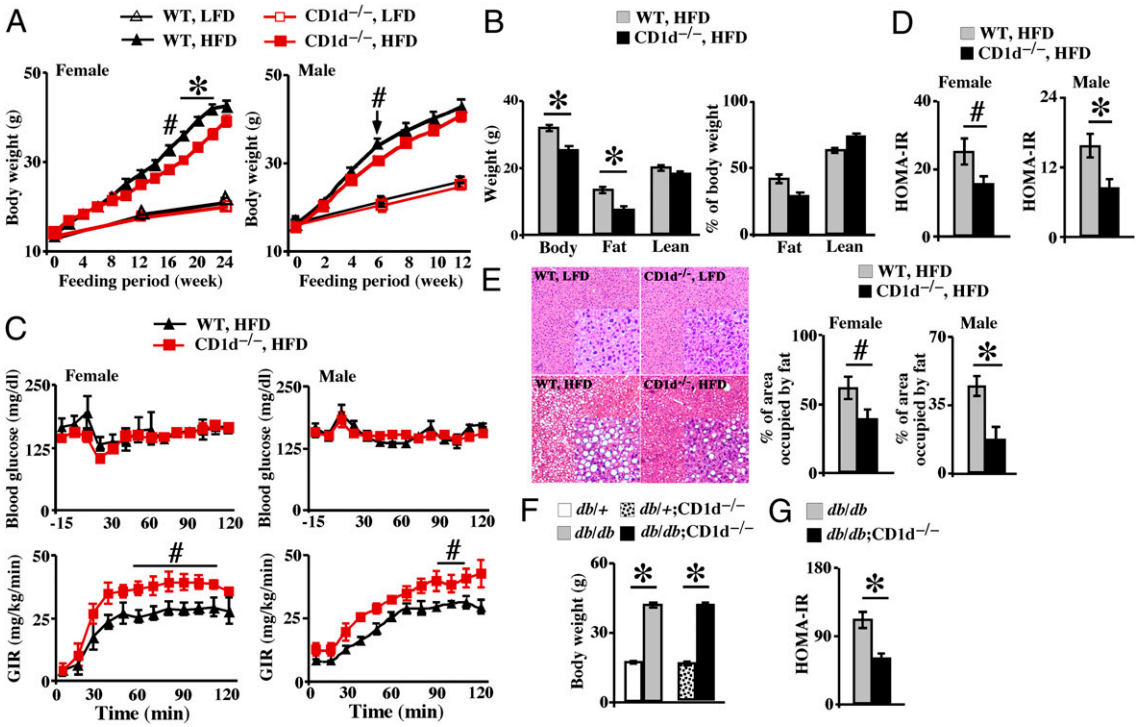

Fig. 4. Effects of *CD1d* deficiency on obesity-induced insulin resistance and hepatic steatosis in mice with DIO or genetic obesity. (*A*) Mice on the B6 background and of the indicated sex and genotypes were fed test diets for the indicated durations and were monitored for body weight. Results are a summary of more than three independent experiments ($n > 10$ in LFD groups and $n > 15$ in HFD groups). (*B*) Female mice of the indicated genotypes were fed the HFD for 12–14 wk and were analyzed for body composition. Results are a summary of three independent experiments ($n = 11$). (*C*) Mice of the indicated sex and genotypes were fed the HFD for 12–14 wk (females) or 10 wk (males) and used for hyperinsulinemic-euglycemic clamp studies. (*Upper*) Maintenance of euglycemia during the assay is demonstrated. (*Lower*) Glucose infusion rates (GIR) are shown. Results are a summary of three independent experiments ($n = 4$ in male experiments; $n = 4$–5 in female experiments). Mice of the indicated sex and genotypes were fed test diets for 20–24 wk (females) or 10–12 wk (males) and killed at fasting state for measurements of HOMA-IR (*D*) and liver lipid accumulation (*E*). Results are a summary of three independent experiments (HFD-fed WT, $n = 10$; HFD-fed *CD1d*$^{-/-}$, $n = 8$). *db*/$^{+}$ and *db*/*db* mice on the B6 background and of the indicated genotypes were fed the RCD and monitored for body weight (*F*), and killed at 15 wk of age at fasting state for determination of HOMA-IR (*G*). Results are a summary of three independent experiments (*db*/*db*, $n = 9$; *db*/*db*;*CD1d*$^{-/-}$, $n = 8$). $^{\#}P < 0.05$; $^{*}P < 0.01$. (Magnification: *E*, 4×; *Insets*, 10×.)

findings have identified iNKT cells as a previously undescribed link between lipid accumulation and chronic inflammation, and therefore place iNKT cells into the complex interplay among immune and parenchymal cells in multiple tissues that are relevant to obesity-triggered inflammation.

iNKT cells harbor properties of both innate and adaptive immune cells, and functionally bridge the innate and adaptive immune systems (13, 33). The semiinvariant TCR on iNKT cells endows these cells with antigen specificity but restricts their reactivity to a limited array of lipid antigens, a property that is reminiscent of the pattern recognition receptors of innate immune cells. In addition to their reactivity to exogenous and endogenous lipid antigens, iNKT cells respond to other lipid stimuli, such as ligands of Toll-like receptors (TLRs). Another innate characteristic of iNKT cells is their capacity to produce large amounts of cytokines rapidly following stimulation, resulting in the release of a mixture of cytokines with both pro- and antiinflammatory properties. Our results indicate that iNKT cells are activated by dietary lipid excess before or around the time of increases in several types of inflammatory leukocytes in liver and WAT. These cells progressively produced increased levels of proinflammatory cytokines and caused an imbalanced proinflammatory cytokine environment in multiple tissues. Consistent with this notion, we found that iNKT cell deficiency ameliorated obesity-induced inflammation, insulin resistance, and excessive lipid accumulation in liver. Conversely, chronic stimulation of iNKT cells with α-GalCer in the context of obesity exacerbated such abnormalities. The consistent results for the *Jα18*$^{-/-}$ and *CD1d*$^{-/-}$ mouse models point toward iNKT cells among NKT cell populations as the main culprits. Our findings support a previous report suggesting a pathogenic role of NKT cells in HFD-induced WAT inflammation using β_2-microglobulin–deficient mice (26) but are inconsistent with two recent reports using *CD1d*$^{-/-}$ mice that failed to observe protection of NKT cell deficiency against HFD-induced metabolic disorders and tissue inflammation (34, 35). The reasons for such discrepancies are unclear, but possible contributing factors include differences in diet composition, feeding duration, and indigenous microbiota in different animal facilities.

The specific stimuli acting on iNKT cells in obesity need further investigation. Our consistent observations in DIO and leptin receptor-deficient *db*/*db* models make it unlikely that leptin and/or leptin-regulated factors play an important role (36). The rapid response of iNKT cells to dietary lipid excess precedes detectable rises in blood TGs, total CHO, and total FFAs, suggesting that these metabolic alterations are unlikely to be responsible for the observed effects. Nevertheless, this does not rule out the possibility that certain FFAs or self-lipids accumulate in obesity and act on iNKT cells. The direct pathway of iNKT cell activation requires recognition of exogenous glycolipid antigens by the TCR. It is unlikely that exogenous glycolipids are involved in our study because iNKT cell alterations were detected in both HFD-fed WT mice and RCD-fed *db*/*db* mice. Alternatively, iNKT cells might become activated via APC-derived proinflammatory cytokines on interaction of certain FFAs with TLRs (37–40). Such a proposed indirect mechanism of iNKT cell activation during obesity might be either dependent or independent of engagement of the TCR with CD1d-

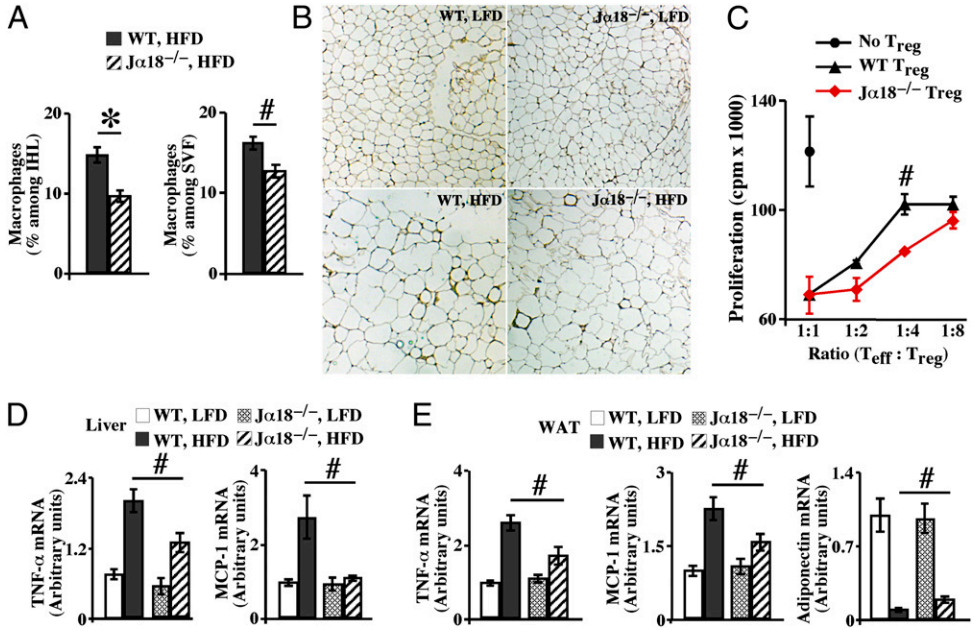

Fig. 5. Effects of iNKT cell deficiency on HFD-induced tissue inflammation. (*A*) Male mice of the indicated genotypes were fed test diets for 10 wk. Macrophages were quantified among IHLs and SVF. Combined data from two independent experiments are shown (HFD-fed WT, $n = 8$; HFD-fed *Jα18*$^{-/-}$, $n = 10$). (*B*) Mice of the indicated genotypes were fed test diets for 20 wk. Paraffin-embedded WAT sections were stained for F4/80. Representative images from two independent experiments ($n = 4$ in LFD groups and $n \geq 8$ in HFD groups) are shown. (Magnification: 20×.) (*C*) Mice of the indicated genotypes were fed the HFD for 10–12 wk. Splenic DCs, T_{eff} cells, and T_{reg} cells were used for the suppression assay. Results are representative data from two independent experiments using five to seven mice in each group per experiment. Female mice of the indicated genotypes were fed test diets for 20 wk. The levels of cytokine and adipokine transcripts in liver (*D*) and WAT (*E*) were examined by real-time PCR. Combined data from three independent experiments ($n \geq 8$ in each treatment group) are shown. $^{\#}P < 0.05$; $^{*}P < 0.01$.

loaded endogenous glycolipids, as previously observed for activation of iNKT cells by microbes (41–44). An attractive possibility is that dyslipidemia in obesity modulates the loading of CD1d with accumulated self-lipids, a scenario supported by a number of studies that have investigated the response of iNKT cells to inflammatory stimuli (41, 42, 45–49). Furthermore, dyslipidemia may also alter the levels of lipid binding/transfer proteins, such as apolipoprotein E, which has been shown to facilitate the delivery and presentation of glycolipids to iNKT cells (50). In preliminary studies, we observed increases in surface CD1d expression on APCs of HFD-fed WT mice (Fig. S9), which provides yet another possible explanation for iNKT cell activation. Finally, it is possible that iNKT cells become activated in response to obesity-induced alterations in neurotransmitters, akin to the activation of hepatic iNKT cells that has been observed in a mouse model of stroke (51). Whatever the iNKT cell stimuli are, our results indicate that the absence of these cells can dissociate lipid accumulation from activation of inflammatory responses in obesity, and therefore ameliorate obesity-associated metabolic diseases.

Another area that requires further investigation is the interaction between iNKT cells and APCs, including macrophages. In the reported pathways of activation, iNKT cells obtain assistance from APCs. Reciprocally, iNKT cells influence the function of APCs and a variety of other leukocytes (13, 14). Our results show that activation of iNKT cells after HFD feeding occurs before or around the time that increases in tissue macrophages are observed. This does not exclude the possibility that rapid uptake of lipids by resident macrophages plays a role in iNKT cell activation (52). This is supported by our preliminary observations that HFD feeding induces increases in CD1d expression on APCs (Fig. S9). These APCs may therefore have increased capacity to present accumulated self-lipids to iNKT cells. Such an intricate interplay between iNKT cells and APCs might provide the driving force to sustain the chronic inflammatory process in obesity.

Our results from chronic α-GalCer treatment are in line with observations in mouse models of atherosclerosis (53–55) and suggest that such treatment exacerbates obesity-associated metabolic diseases. Because obesity and atherosclerosis share a common feature of hyperlipidemia, these findings are consistent with the lipid-reactive nature of iNKT cells.

In conclusion, our findings provide evidence that lipid excess in obesity activates iNKT cells and that these cells contribute to the development of obesity-induced inflammation, insulin resistance, and hepatic steatosis. Our findings therefore place iNKT cells within the complex network that links lipid excess to obesity-induced inflammation and suggest potential therapeutic avenues for obesity-associated metabolic disorders. For example, our findings suggest that selective depletion of iNKT cells with an iNKT cell-specific antibody (56) might be beneficial in protecting human subjects from obesity-associated metabolic disease.

Methods

Mice. We used WT B6 mice, *db/db* and *db/*$^{+}$ mice on the B6 background (Jackson Laboratory), and *Jα18*$^{-/-}$ and *CD1d*$^{-/-}$ mice on the B6 background (both were backcrossed to B6 for greater than 10 generations) (29, 57). The *db/*$^{+}$ mice were bred with *Jα18*$^{-/-}$ or *CD1d*$^{-/-}$ mice to generate *db/db;Jα18*$^{-/-}$ and *db/db;CD1d*$^{-/-}$ mice on the B6 background. Sex- and age-matched animals between experimental and control groups were used in each experiment and were housed under specific pathogen-free conditions. In studies using *Jα18*$^{-/-}$ and *CD1d*$^{-/-}$ mice, both WT littermates of the mutant mice and WT mice from the Jackson Laboratory were examined. The experimental procedures were approved by the Institutional Animal Care and Use Committee of Vanderbilt University Medical Center.

Diets. We fed mice the RCD (Labdiet; catalogue no. 5001), LFD (Bio-serv; catalogue no. F4031), or HFD (Bio-serv; catalogue no. F3282), using lard as the fat source. Dietary manipulation began when mice were 5–6 wk of age and continued for the periods indicated in *Results* and figure legends.

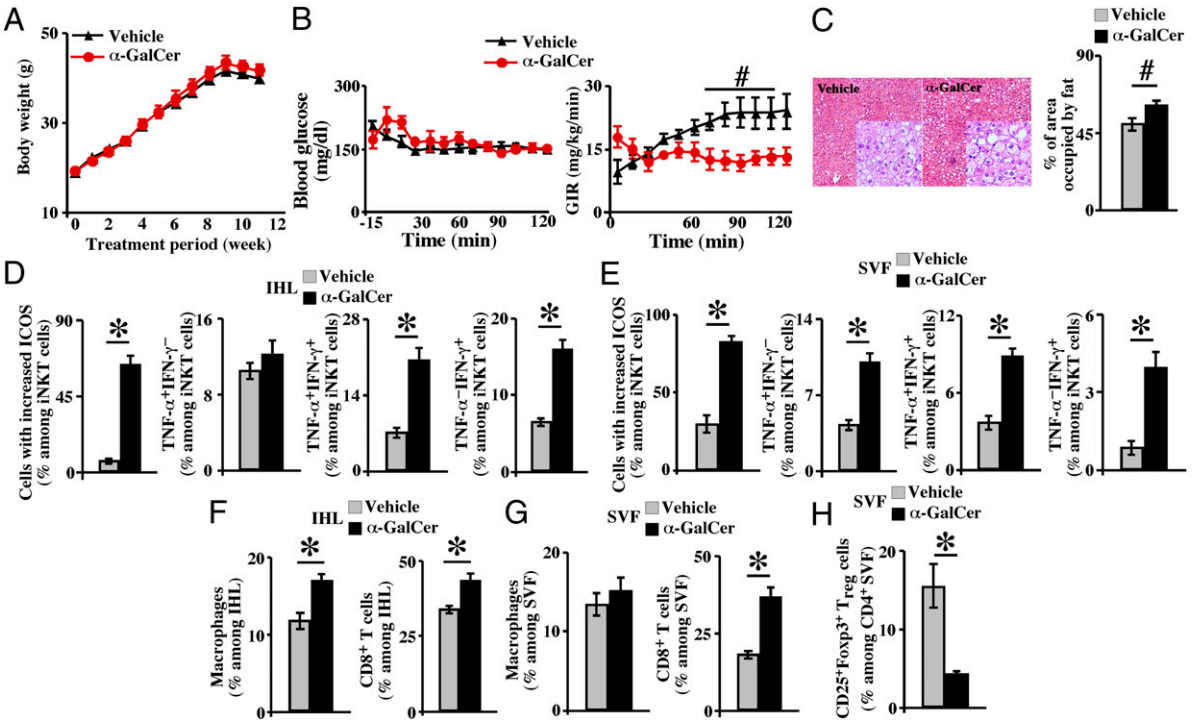

Fig. 6. Effects of chronic α-GalCer treatment on DIO. Male WT B6 mice were fed the HFD and injected i.p. with vehicle or α-GalCer at 1 μg per mouse per week for 8 wk. (*A*) Body weight was monitored weekly ($n = 10$ in each treatment group). (*B*) Insulin sensitivity was examined 2 wk after the last injection by hyperinsulinemic-euglycemic clamp ($n = 4$ in each treatment group). Mice were killed 2–3 wk after the last injection for measurement of liver lipid accumulation (*C*), ICOS expression on hepatic iNKT cells (*D*) and WAT iNKT cells (*E*), cytokines in hepatic iNKT cells (*D*) and WAT iNKT cells (*E*), macrophages and $CD8^+$ T cells among IHLs (*F*) and SVFs (*G*), and $CD25^+Foxp3^+$ T_{reg} cells among $CD4^+$ T cells in SVFs (*H*). Combined data from two independent experiments with five mice in each group per experiment are shown in *C–H*. $^{\#}P < 0.05$; $^{*}P < 0.01$. (Magnification: *C*, 4×; *Insets*, 10×.)

Reagents. α-GalCer (KRN7000) was kindly provided by Kirin Brewery Co. or purchased from Funakoshi Co., and the synthesis of C20:2 has been described (58). Mouse CD1d monomers were from the National Institutes of Health Tetramer Facility and were used to prepare α-GalCer/CD1d-tetramers (59). We used fluorescently labeled antibodies (BD Biosciences or Ebioscience) against mouse TCR-β, CD19, CD11b, CD11c, F4/80, CD8-α, CD4, CD44, CD62L, ICOS, NK1.1, CD69, CD40L, CD25, IFN-γ, IL-4, TNF-α, Foxp3, and CD1d, and mouse CD1d-tetramers for surface and/or intracellular labeling. OptEIA sets were purchased from BD Biosciences. We purchased purified anti-mouse F4/80 from Invitrogen and a Vectastain ABC kit from Vector Labs for F4/80 immunocytochemistry.

Cell Preparation and Culture. We analyzed iNKT cells in liver, WAT, and spleen simultaneously in each mouse. IHLs were purified from liver using collagenase IV (Sigma) digestion and Percoll (GE Healthcare) centrifugation (60, 61). SVF cells were purified from mouse perigonadal fat pads using collagenase I (Worthington Biochemical Corporation) digestion (62). RBCs were lysed using ACK buffer (Lonza). Ex vivo cultures were performed at a density of 1×10^5 cells per well for IHLs and at 2×10^5 cells per well for splenocytes, as described (61). Cells were cultured ex vivo in the absence or presence of α-GalCer for 72 h at concentrations specified in each assay.

Responses of iNKT Cells to Acute in Vivo Challenge with α-GalCer. Mice were injected i.p. with either vehicle (PBS containing 0.025% polysorbate-20) or α-GalCer and were killed 2 h later for isolation of SVFs as described and of IHLs as described without collagenase IV digestion (61). In long-term HFD-fed mice, we used α-GalCer at 50 ng/g of body weight to compensate for the differences in body weights. In mice on diets for 1 wk, we used 2 μg of α-GalCer per mouse as described (61). Isolated cells were cultured for 2–3 h with Golgi-plug (BD Biosciences) and used for subsequent surface and intracellular staining.

Surface and Intracellular Staining and Flow Cytometric Analyses. We labeled mouse iNKT cells as previously described (28, 61). iNKT cells were characterized as $CD19^-TCR\text{-}\beta^{low}$α-GalCer/CD1d-tetramer$^+$ cells. Macrophages were identified as $CD11b^+F4/80^+$ cells, and DCs were identified as $CD11b^-CD11c^+$ cells. $CD8^+$ T cells were identified as $CD19^-TCR\text{-}\beta^+CD8\text{-}\alpha^+CD4^-$ cells. $CD8^+$ effector T cells were identified as $CD44^+CD62L^-$ cells among $CD19^-TCR\text{-}\beta^+CD8\text{-}\alpha^+CD4^-$ cells. T_{reg} cells were identified as $CD4^+CD25^+Foxp3^+$ cells. Surface activation markers were examined among gated iNKT cells. Intracellular labeling of cytokines in iNKT cells and of Foxp3 in IHLs and SVF cells was performed as described (61). Flow cytometry was performed using a FACSCalibur (BD Biosciences) with FSC set on a linear scale and SSC set on a log scale using CellQuest software (BD Biosciences–Immunocytometry Systems). The acquired data were analyzed using FlowJo software (Tree Star, Inc.).

Cytokine ELISA. Supernatants of cultured IHLs, SVF cells, or splenocytes were harvested after 72 h of culture and stored at −80 °C. A standard sandwich ELISA was performed to measure mouse IFN-γ, IL-4, IL-10, IL-12, TNF-α, and IL-6.

Metabolic Parameters. Body weight and body composition (mq10 NMR analyzer; Bruker Optics) were measured between 9:00 and 10:00 AM. Energy expenditure (Oxymax indirect calorimetry system; Columbus Instruments) and food intake were examined as described (63). Hyperinsulinemic-euglycemic clamps were performed by the isotope dilution method in conscious mice with indwelling catheters in a carotid artery and a jugular vein using an unprimed insulin infusion of 4 milliunits (mU)·kg·min as described (63). Clamps were conducted for 120 min, during which time arterial glucose was measured at 10-min intervals to provide feedback on which the variable rate of glucose infusion was based. The steady-state period was defined by stable glycemia during the last 40 min of the clamp period. Blood glucose (Accu-chek), insulin (Crystal Chem), TGs, CHO, and FFAs (Wako) were examined after 14 h of fasting. An IPITT was performed after 6 h of fasting using a bolus i.p. injection of insulin at 2 units/kg of body weight, followed by glucose sampling through the saphenous vein. HOMA-IR was calculated according to the following formula: fasting blood glucose (mmol/L) × fasting blood insulin (mU/L)/22.5.

Quantitative Real-Time PCR. Mouse liver and WAT were snap-frozen at sacrifice and stored at −80 °C. We measured mRNA levels of cytokines and adipokines as described (64, 65).

In Vivo Stimulation with α-GalCer and Evaluation of iNKT Cell Expansion and Cytokine Expression in WAT. Mice were injected i.p. with either vehicle or α-GalCer (1 μg per mouse) and killed 3 d later. WAT was either used for quantification of iNKT cells in isolated SVFs or snap-frozen and stored at −80 °C for real-time PCR analyses of cytokines.

Chronic Glycolipid Treatment. Mice were placed on the HFD when they were 5–6 wk of age. Vehicle, α-GalCer, or C20:2 (1 μg per mouse per injection) was injected i.p. once a week for 8 wk. Mice were examined 2–3 wk after the last injection. Both IHLs and SVFs were prepared using collagenase digestion and used for surface and intracellular labeling as described above.

Liver Lipids and Adipocyte Size. Liver lipids were extracted from frozen liver tissue, and TG content was measured by gas chromatography as described (66). For histological grading of liver lipids and adipocyte size, liver and WAT were fixed in formalin and processed for paraffin-embedded sections. H&E-stained liver or WAT sections were viewed under a Leica inverted microscope. Five images were taken from each mouse at magnifications of 4× and 10× (liver) or 20× (WAT). The areas occupied by lipids in hepatocytes on liver sections and the areas covered by adipocytes on WAT sections were quantified using National Institutes of Health ImageJ software.

F4/80 Staining in WAT. WAT sections prepared as above were stained with F4/80 as described (66) and visualized under a Leica inverted microscope.

Purification and Culture of Leukocytes from SVFs. SVFs were isolated as described above from mouse WAT. Leukocytes were sorted by preparative flow cytometry based on their FSC/SSC distribution using a FACSAria III cell sorter (BD Biosciences). Doublets were excluded from the analyses using light scatter pulse-processed data based on sequential gating on SSC-W vs. SSC-H and FSC-W vs. FSC-H (W, width; H, height). Sorted cells were cultured at a density of ∼1 × 10^5 per well in the absence or presence of 50 ng/mL α-GalCer for 72 h. Supernatants were collected at the end of culture and stored at −80 °C for further analyses of cytokines by ELISA.

Functional Assay of T_{reg} Cells. CD11c$^+$ DCs, CD4$^+$CD25$^-$ effector T (T_{eff}) cells, and CD4$^+$CD25$^+$ T_{reg} cells were purified from splenocytes by magnetic activated cell sorting using reagents from Miltenyi Biotechnology. Isolated cells were subsequently cultured for 72 h at densities of 2 × 10^5 T_{eff} cells, 4 × 10^4 DCs, and varying numbers of T_{reg} cells, and were stimulated with plate-bound anti-CD3ε. Cell proliferation was measured by a ^{3}H-thymidine (PerkinElmer) incorporation assay.

Statistical Analyses. The numbers in each assay represent the numbers of mice examined, except for the SVFs from lean mice in which fat pads from three mice were pooled and counted as one sample. Data are presented as means ± SEM. Statistical analyses were performed using an unpaired two-tailed *t* test after examining distribution normality of the data. A *P* value less than 0.05 was considered statistically significant.

ACKNOWLEDGMENTS. We thank the Kirin Brewery Co. for providing KRN7000; the National Institutes of Health (NIH) tetramer facility for CD1d monomers; Dr. M. Taniguchi for *Jα18*-deficient mice; the Vanderbilt Mouse Metabolic Phenotyping Center (supported by NIH Grant U24 DK59637) for support with the metabolic studies; and Drs. Sebastian Joyce, Jacek Hawiger, and Alvin C. Powers for helpful discussions. This work was supported by a Junior Faculty Award from the American Diabetes Association (to L.W.); a Pilot and Feasibility Grant from the Diabetes Research and Training Center at Vanderbilt University (to L.W.); NIH Grants DK081536 (to L.W. and L.V.K.), AI070305 (to L.V.K.), HL089667 (to L.V.K.), and DK50277 (to D.H.W.); a personal research chair from James Bardrick (to G.S.B.); a Royal Society Wolfson Research Merit Award (to G.S.B.); the Medical Research Council (G.S.B.); the Wellcome Trust (G.S.B.); a postdoctoral fellowship from the National Multiple Sclerosis Society (to V.V.P.); an individual predoctoral fellowship from NIH (to C.L.G.); and a postdoctoral fellowship from the Irvington Institute Fellowship Program of the Cancer Research Institute (to Y.V.M.-F.).

1. Gregor MF, Hotamisligil GS (2011) Inflammatory mechanisms in obesity. *Annu Rev Immunol* 29:415–445.
2. Shoelson SE, Lee J, Goldfine AB (2006) Inflammation and insulin resistance. *J Clin Invest* 116:1793–1801.
3. Schenk S, Saberi M, Olefsky JM (2008) Insulin sensitivity: Modulation by nutrients and inflammation. *J Clin Invest* 118:2992–3002.
4. Qatanani M, Lazar MA (2007) Mechanisms of obesity-associated insulin resistance: Many choices on the menu. *Genes Dev* 21:1443–1455.
5. Lumeng CN, Bodzin JL, Saltiel AR (2007) Obesity induces a phenotypic switch in adipose tissue macrophage polarization. *J Clin Invest* 117:175–184.
6. Odegaard JI, Chawla A (2008) Mechanisms of macrophage activation in obesity-induced insulin resistance. *Nat Clin Pract Endocrinol Metab* 4:619–626.
7. Winer S, et al. (2009) Normalization of obesity-associated insulin resistance through immunotherapy. *Nat Med* 15:921–929.
8. Nishimura S, et al. (2009) CD8$^+$ effector T cells contribute to macrophage recruitment and adipose tissue inflammation in obesity. *Nat Med* 15:914–920.
9. Feuerer M, et al. (2009) Lean, but not obese, fat is enriched for a unique population of regulatory T cells that affect metabolic parameters. *Nat Med* 15:930–939.
10. Winer DA, et al. (2011) B cells promote insulin resistance through modulation of T cells and production of pathogenic IgG antibodies. *Nat Med* 17:610–617.
11. Kronenberg M (2005) Toward an understanding of NKT cell biology: Progress and paradoxes. *Annu Rev Immunol* 23:877–900.
12. Bendelac A, Savage PB, Teyton L (2007) The biology of NKT cells. *Annu Rev Immunol* 25:297–336.
13. Van Kaer L (2007) NKT cells: T lymphocytes with innate effector functions. *Curr Opin Immunol* 19:354–364.
14. Matsuda JL, Mallevaey T, Scott-Browne J, Gapin L (2008) CD1d-restricted iNKT cells, the 'Swiss-Army knife' of the immune system. *Curr Opin Immunol* 20:358–368.
15. Caspar-Bauguil S, et al. (2005) Adipose tissues as an ancestral immune organ: Site-specific change in obesity. *FEBS Lett* 579:3487–3492.
16. Lynch L, et al. (2009) Invariant NKT cells and CD1d(+) cells amass in human omentum and are depleted in patients with cancer and obesity. *Eur J Immunol* 39:1893–1901.
17. Godfrey DI, MacDonald HR, Kronenberg M, Smyth MJ, Van Kaer L (2004) NKT cells: What's in a name? *Nat Rev Immunol* 4:231–237.
18. Borg NA, et al. (2007) CD1d-lipid-antigen recognition by the semi-invariant NKT T-cell receptor. *Nature* 448:44–49.
19. MacDonald HR (2000) CD1d-glycolipid tetramers: A new tool to monitor natural killer T cells in health and disease. *J Exp Med* 192:F15–F20.
20. Jahng A, et al. (2004) Prevention of autoimmunity by targeting a distinct, noninvariant CD1d-reactive T cell population reactive to sulfatide. *J Exp Med* 199: 947–957.
21. Li Z, et al. (2004) Norepinephrine regulates hepatic innate immune system in leptin-deficient mice with nonalcoholic steatohepatitis. *Hepatology* 40:434–441.
22. Li Z, Soloski MJ, Diehl AM (2005) Dietary factors alter hepatic innate immune system in mice with nonalcoholic fatty liver disease. *Hepatology* 42:880–885.
23. Yang L, Jhaveri R, Huang J, Qi Y, Diehl AM (2007) Endoplasmic reticulum stress, hepatocyte CD1d and NKT cell abnormalities in murine fatty livers. *Lab Invest* 87: 927–937.
24. Elinav E, et al. (2006) Adoptive transfer of regulatory NKT lymphocytes ameliorates non-alcoholic steatohepatitis and glucose intolerance in ob/ob mice and is associated with intrahepatic CD8 trapping. *J Pathol* 209:121–128.
25. Miyazaki Y, et al. (2008) Effect of high fat diet on NKT cell function and NKT cell-mediated regulation of Th1 responses. *Scand J Immunol* 67:230–237.
26. Ohmura K, et al. (2010) Natural killer T cells are involved in adipose tissues inflammation and glucose intolerance in diet-induced obese mice. *Arterioscler Thromb Vasc Biol* 30:193–199.
27. Koller BH, Marrack P, Kappler JW, Smithies O (1990) Normal development of mice deficient in β 2M, MHC class I proteins, and CD8$^+$ T cells. *Science* 248:1227–1230.
28. Wilson MT, et al. (2003) The response of natural killer T cells to glycolipid antigens is characterized by surface receptor down-modulation and expansion. *Proc Natl Acad Sci USA* 100:10913–10918.
29. Mendiratta SK, et al. (1997) CD1d1 mutant mice are deficient in natural T cells that promptly produce IL-4. *Immunity* 6:469–477.
30. Yu KO, et al. (2005) Modulation of CD1d-restricted NKT cell responses by using N-acyl variants of alpha-galactosylceramides. *Proc Natl Acad Sci USA* 102:3383–3388.
31. Lumeng CN, Maillard I, Saltiel AR (2009) T-ing up inflammation in fat. *Nat Med* 15: 846–847.
32. Shoelson SE, Goldfine AB (2009) Getting away from glucose: Fanning the flames of obesity-induced inflammation. *Nat Med* 15:373–374.
33. Bendelac A, Bonneville M, Kearney JF (2001) Autoreactivity by design: Innate B and T lymphocytes. *Nat Rev Immunol* 1:177–186.
34. Mantell BS, et al. (2011) Mice lacking NKT cells but with a complete complement of CD8$^+$ T-cells are not protected against the metabolic abnormalities of diet-induced obesity. *PLoS ONE* 6:e19831.
35. Kotas ME, et al. (2011) Impact of CD1d deficiency on metabolism. *PLoS ONE* 6:e25478.
36. Faggioni R, Feingold KR, Grunfeld C (2001) Leptin regulation of the immune response and the immunodeficiency of malnutrition. *FASEB J* 15:2565–2571.
37. Nguyen MT, et al. (2007) A subpopulation of macrophages infiltrates hypertrophic adipose tissue and is activated by free fatty acids via Toll-like receptors 2 and 4 and JNK-dependent pathways. *J Biol Chem* 282:35279–35292.
38. Hwang D (2001) Modulation of the expression of cyclooxygenase-2 by fatty acids mediated through toll-like receptor 4-derived signaling pathways. *FASEB J* 15: 2556–2564.
39. Lee JY, Sohn KH, Rhee SH, Hwang D (2001) Saturated fatty acids, but not unsaturated fatty acids, induce the expression of cyclooxygenase-2 mediated through Toll-like receptor 4. *J Biol Chem* 276:16683–16689.
40. Shi H, et al. (2006) TLR4 links innate immunity and fatty acid-induced insulin resistance. *J Clin Invest* 116:3015–3025.
41. Mattner J, et al. (2005) Exogenous and endogenous glycolipid antigens activate NKT cells during microbial infections. *Nature* 434:525–529.

42. Brigl M, Bry L, Kent SC, Gumperz JE, Brenner MB (2003) Mechanism of CD1d-restricted natural killer T cell activation during microbial infection. *Nat Immunol* 4:1230–1237.
43. Nagarajan NA, Kronenberg M (2007) Invariant NKT cells amplify the innate immune response to lipopolysaccharide. *J Immunol* 178:2706–2713.
44. Tyznik AJ, et al. (2008) Cutting edge: The mechanism of invariant NKT cell responses to viral danger signals. *J Immunol* 181:4452–4456.
45. Paget C, et al. (2007) Activation of invariant NKT cells by toll-like receptor 9-stimulated dendritic cells requires type I interferon and charged glycosphingolipids. *Immunity* 27:597–609.
46. Salio M, et al. (2007) Modulation of human natural killer T cell ligands on TLR-mediated antigen-presenting cell activation. *Proc Natl Acad Sci USA* 104: 20490–20495.
47. Fox LM, et al. (2009) Recognition of lyso-phospholipids by human natural killer T lymphocytes. *PLoS Biol* 7:e1000228.
48. Muindi K, et al. (2010) Activation state and intracellular trafficking contribute to the repertoire of endogenous glycosphingolipids presented by CD1d [corrected]. *Proc Natl Acad Sci USA* 107:3052–3057.
49. Brennan PJ, et al. (2011) Invariant natural killer T cells recognize lipid self antigen induced by microbial danger signals. *Nat Immunol* 12:1202–1211.
50. van den Elzen P, et al. (2005) Apolipoprotein-mediated pathways of lipid antigen presentation. *Nature* 437:906–910.
51. Wong CH, Jenne CN, Lee WY, Léger C, Kubes P (2011) Functional innervation of hepatic iNKT cells is immunosuppressive following stroke. *Science* 334:101–105.
52. Lichtenstein L, et al. (2010) Angptl4 protects against severe proinflammatory effects of saturated fat by inhibiting fatty acid uptake into mesenteric lymph node macrophages. *Cell Metab* 12:580–592.
53. Nakai Y, et al. (2004) Natural killer T cells accelerate atherogenesis in mice. *Blood* 104: 2051–2059.
54. Major AS, et al. (2004) Quantitative and qualitative differences in proatherogenic NKT cells in apolipoprotein E-deficient mice. *Arterioscler Thromb Vasc Biol* 24:2351–2357.
55. Tupin E, et al. (2004) CD1d-dependent activation of NKT cells aggravates atherosclerosis. *J Exp Med* 199:417–422.
56. Exley MA, et al. (2008) Selective activation, expansion, and monitoring of human iNKT cells with a monoclonal antibody specific for the TCR alpha-chain CDR3 loop. *Eur J Immunol* 38:1756–1766.
57. Cui J, et al. (1997) Requirement for Valpha14 NKT cells in IL-12-mediated rejection of tumors. *Science* 278:1623–1626.
58. Jervis PJ, et al. (2010) Synthesis and biological activity of alpha-glucosyl C24:0 and C20: 2 ceramides. *Bioorg Med Chem Lett* 20:3475–3478.
59. Stanic AK, et al. (2003) Defective presentation of the CD1d1-restricted natural Va14Ja18 NKT lymphocyte antigen caused by β-D-glucosylceramide synthase deficiency. *Proc Natl Acad Sci USA* 100:1849–1854.
60. Crispe IN (1997) Isolation of mouse intrahepatic lymphocytes. *Curr Protoc Immunol* 1: 3.21.21–23.21.28.
61. Parekh VV, et al. (2005) Glycolipid antigen induces long-term natural killer T cell anergy in mice. *J Clin Invest* 115:2572–2583.
62. Wu D, et al. (2007) Aging up-regulates expression of inflammatory mediators in mouse adipose tissue. *J Immunol* 179:4829–4839.
63. Ayala JE, et al. (2007) Chronic treatment with sildenafil improves energy balance and insulin action in high fat-fed conscious mice. *Diabetes* 56:1025–1033.
64. Furuhashi M, et al. (2008) Adipocyte/macrophage fatty acid-binding proteins contribute to metabolic deterioration through actions in both macrophages and adipocytes in mice. *J Clin Invest* 118:2640–2650.
65. Chen QY, et al. (2010) Human CD1D gene expression is regulated by LEF-1 through distal promoter regulatory elements. *J Immunol* 184:5047–5054.
66. Ellacott KL, Murphy JG, Marks DL, Cone RD (2007) Obesity-induced inflammation in white adipose tissue is attenuated by loss of melanocortin-3 receptor signaling. *Endocrinology* 148:6186–6194.